Available online at www.sciencedirect.com
SCIENCE DIRECT®
Journal of Hydrology 278 (2003) 153–171
Journal of Hydrology
www.elsevier.com/locate/jhydrol

Hyporheic exchange of reactive and conservative solutes in streams—tracer methodology and model interpretation

Karin Jonsson[a,*], Håkan Johansson[b], Anders Wörman[b]

[a]Department of Earth Sciences, Uppsala University, Villavägen 16, SE-752 36 Uppsala, Sweden
[b]Department of Biometry and Informatics, Swedish University of Agricultural Sciences, P.O. Box 7013, SE-75007 Uppsala, Sweden

Received 2 July 2002; accepted 28 March 2003

Abstract

A transient storage model is evaluated using results from a tracer experiment, where a conservative and a reactive tracer (^{3}H and $^{51}Cr(III)$) were injected simultaneously and monitored in stream water and bed sediment. About 76% of the chromium was lost from the stream water on the reach 30 km downstream of the injection point directly after the passage of the pulse in the flowing water. The bed sediment hosted the main part of the retained chromium. The time to washout 75% of the maximum solute uptake in the sediment was ~85 times longer for chromium than for tritium (i.e. ~45 days). It was possible to describe the sediment-water exchange with a diffusive flux formulation that could be evaluated using tritium breakthrough curves in the stream water or the tritium inventory breakthrough curves in the sediment. This experiment revealed further that observations of chromium concentrations in the sediment were essential for the quantifying of sorption properties, as it was not possible to catch accurately the time scale of sorption within the duration of the breakthrough curves in the stream water. There was a clear need for a rate-limited description of the sorption of chromium in the sediment. We found that a first-order kinetic description of the sorption process could acceptably describe the breakthrough curves in both the stream water and the bed sediment.

Keywords: Model; Sorption kinetics; Sediment; Stream; Tracer experiment; Transient storage

1. Introduction

The continuous exchange of water between stream water and underlying sediment is an important process determining the fate of contaminants. Pressure-driven advection, arising due to irregularities on the sediment surface, is believed to be an important hydraulic mechanism that causes the stream water to flow into and out of stream beds (Thibodeaux and Boyle, 1987).

In addition to the continuous filtration of stream water through bed sediment, numerous chemical reactions influence the net exchange of reactive substances between the sediment and the overlaying stream water. A large portion of reactive contaminants in solution can be captured within the sediment due to adsorption on to particulate matter. Later on, the contaminants, depending on the sorption characteristics, can eventually be partly or totally released back into the water column.

Models for the hyporheic exchange of solutes in rivers and streams are usually supported by tracer experiments (Bencala and Walters, 1983; Jackman

* Corresponding author.
E-mail address: karin.jonsson@geo.uu.se (K. Jonsson).

0022-1694/03/$ - see front matter © 2003 Elsevier Science B.V. All rights reserved.
doi:10.1016/S0022-1694(03)00140-9

et al., 1984; Harvey et al., 1996; Wörman et al., 1998; Hart et al., 1999). Model descriptions of solute transport generally include advection, dispersion and exchange from the streaming water to one or several storage zones. The exchange is often described as a first-order loss from the water phase or as a diffusive flux into the surrounding storage zone (Bencala, 1983; Wörman, 2000). To describe the exchange of reactive substances, also the affect of sorption on to particulate matter has to be incorporated in the model formulation. A usual methodology is to fit the model prediction to the breakthrough curves (BTCs) established from tracer experiments or to evaluate the temporal moments of the observed breakthrough curves (Legrand-Marcq and Laudelout, 1985; Bencala et al., 1990; Wörman et al., 1998; Chapra and Wilcock, 2000; Lees et al., 2000; Johansson et al., 2001; Seo and Cheong, 2001).

Many of the experiments reported in the literature are performed with only a single tracer at a time. In order to differentiate between the transport characteristics of a reactive and a conservative substance, it is appropriate to inject simultaneously both solutes. Another usual limitation is that the proposed modelling concept is fitted only to the BTCs in the stream water. In this way parameters for the stream water and the storage zone will be determined without any independent observations of the processes in the storage zone (Bencala et al., 1990; Hart et al., 1999; Lees et al., 2000). A critical test of model validity could include fitting also to the concentration observed in the storage zone. This allows for an independent evaluation of the ability of the models to describe the retardation of a substance along a stream.

Wagner and Harvey (1997) stressed the importance of the sampling methodology and the type of solute injection for a reliable evaluation of the model parameters. They found that a constant solute injection with a rise, plateau and fall gave more reliable parameter estimates than a pulse injection.

The purpose of the present study was to perform and evaluate a simultaneous tracer injection of a conservative (^{3}H as tritiated water) and a reactive (^{51}Cr as Cr(III)) tracer and to monitor the change in solute concentration in both the flowing stream water and the bed sediment along a 30 km reach of the Säva Stream. The investigation period was extended compared to most previous tracer tests to almost half a year.

One essential component of the study was to identify the processes controlling the exchange of the conservative and the reactive substance and further to quantify their relative importance for the solute transport.

A model is developed and fitted to the tracer BTCs with respect to both tritium and chromium in order to quantify the variability of the prevailing processes affecting solute transport along the stream. In order to reveal the importance of independent observations for the quantification of transport parameters, we have evaluated the modelling concept with respect to the observations made in both the stream water and the bed sediment. Thereby it is possible to reveal what kind of field observations are needed to evaluate the hydraulic and chemical processes, respectively.

Johansson et al. (2001) have presented parts of the results of The Säva Stream Tracer Experiment 1998, but here we present a larger amount of data and use this in a more comprehensive evaluation than has previously been done. Especially a cross-validation of the model is ensured by using observations in both flowing water and bed sediment.

2. Experiment

The Säva Stream Tracer Experiment 1998 was performed on 19th of May 1998 along a 30 km-long reach of the Säva Stream, Uppland County, Sweden. A simultaneous injection with a constant rate was performed during 5.3 h using the tracers tritium (74 GBq) and chromium (92.5 GBq). ^{51}Cr(III) was found suitable to represent a reactive tracer due to its known reactivity (Wörman et al., 1998) in combination with a relatively short physical half-life and low energetic gamma-radiation. During the injection, the chromium concentration (including the added non-radioactive Cr(III) carrier substance) in the stream water increased by 0.0001 nM.

In aqueous environment, it is possible that different redox- and precipitation processes might alter the chemical state of the injected chromium and thereby also its uptake potential on to particulate matter. In the present study, where the stream water was slightly humic, it is probable that a large fraction of

the injected Cr(III) can remain in its trivalent oxidation state during the experiment due to photochemical regeneration of Cr(III) via ferrous iron, hydrogen peroxide and dissolved organic carbon and Cr(III)-complexation to dissolved organic carbon (Kieber and Heiz, 1992; Kaczynski and Kieber, 1993; Kaczynski and Kieber, 1994).

Water samples were collected during the passage of the pulse to get complete BTCs at each station. Sediment core samples were collected over a period of several months in order to capture both the uptake and the washout phase of the injected tracers.

To obtain a detailed local mapping of the spatial variability, we collected a plate (lamella) of sediment oriented in the stream water direction and vertically at the first station. The plate was taken approximately 20 h after the passage of the pulse, and the length and depth of the plate were approximately 0.9 m and at least 0.14 m, respectively. The plate was then sectioned into ~100 samples and the concentration of chromium was determined in each sample.

Some sediment core samples were also leached with extraction solvents to get information about chromium's relative association with different 'types' of substrate in the bed sediment (e.g. association with iron and manganese oxides, carbonates, etc.). Due to the field conditions and the need to perform the extractions immediately in the field, a modified version of the extraction Scheme by Riise et al. (1990) and Broberg (1994) was applied. Instead of the sequential extraction procedure with a single sediment sample, sub-samples were leached with each of the extraction solvents for 3 h at a temperature of 20 °C.

Tritium concentration in stream water and pore water was analysed with a beta scintillation counter whereas the chromium concentration in stream water and pore water was analysed with a gamma spectrometer. Since both of the radionuclides decay with time ($t_{1/2}(^{51}\mathrm{Cr}) = 27.703$ days and $t_{1/2}(^{3}\mathrm{H}) = 12.6$ years), all samples were corrected to the time of the start of the injection. See Johansson et al. (2001) for detailed analysis description.

2.1. Experimental results

2.1.1. Water data

Breakthrough curves for tritium and chromium in the stream water were observed at eight stations denoted A, B, C, D, E, F1, F2 and G, located 125; 2100; 5400; 9400; 16,100; 20,600; 21,100 and 29,500 m downstream of the injection point (Fig. 1a and b).

The reason for the close position of stations F1 and F2 is due to a small and shallow pool with dense macrophyte vegetation located between those two stations.

The distortion of the BTCs in the stream water evident from Fig. 1 is due partly to the net exchange taking place with the hyporheic zone along the stream. From a solute mass balance, a 76% loss of chromium was found along the 30 km study reach at the end of the water sampling (+150 h) (Fig. 2).

The sub-reaches A–B and F1–F2 have a relatively high loss of chromium per length metre of the stream (Fig. 2). The explanation to the high loss at sub-reach A–B has not been identified whereas the probably cause at sub-reach F1–F2 is uptake of chromium on to the dense vegetation.

Vegetation sampling during the experiment (although conducted at station A) indicates that the uptake on vegetation can result in high concentrations of chromium expressed on a dry weight basis. The following uptake of chromium was found at station A: (1) surficial sediment ($t = +5.2$ h) 18,000 dpm/g dw (LOI: 9.8%); (2) vegetation surfaces 150,000 dpm/g dw (LOI: 88%) and (3) suspended particulate matter (SPM) attached to vegetation 392,000 dpm/g dw (LOI: 31%). (LOI and dw denote loss on ignition (= organic content) and dry weight, respectively.).

Hence, except for sub-reaches with dense vegetation, it is unlikely that the uptake of chromium on vegetation surfaces (including attached SPM) will contribute to a substantial loss of chromium compared to the large internal surface area of the bed sediment.

According to Johansson et al. (2001), the distribution between adsorbed (c_a, [dpm/m^3]) and dissolved (c_d, [dpm/m^3]) chromium, K_d ($= c_a/c_d$), was found by filtration through a 0.45 μm filter to vary between 0.29–0.31. The pH and the conductivity in the stream water during the experiment were 7.2 and 27.7 mS/m, respectively.

2.1.2. Sediment data

Sediment was sampled at stations A and C. A visual characterization, strengthened by a few number of grain size determinations, revealed that

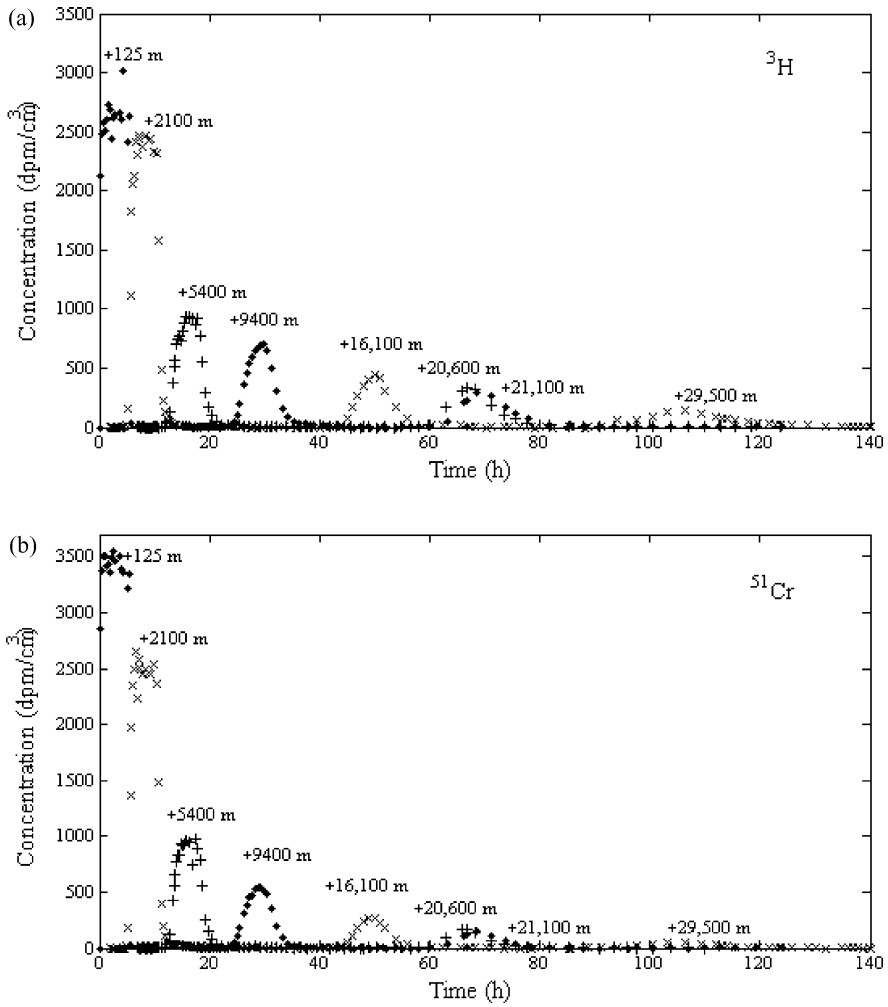

Fig. 1. Breakthrough curves in the stream water at stations A–G (a) tritium (b) chromium.

the sediment consisted of both silt and clay with the latter increasing with distance along the stream. At each occasion 5–7 sediment cores were taken and sectioned by depth (0–1, 1–2, 2–4, 4–7, 7–10, 10–15 and 15–21 cm). Samples from the same depth and sampling occasion were mixed to get arithmetic mean values of the uptake. However, on some occasions, sediment slices from the same depth interval in the different cores were analysed separately. On all sampling occasions, the concentration profiles were measured at least down to 10 cm (corresponding class-mean: 8.5 cm). From the depth profiles we can conclude that most of the solute mass in the sediment is located in the uppermost 10 cm (Figs. 3 and 4).

It is apparent that the time scales for uptake and washout differ between chromium and tritium (Figs. 3, 5 and 6). The depth profile for tritium after 168 h reveals that the washout is practically complete, whereas for chromium the concentration has not reached the background value even after 1510 h, implying that the washout is still in progress (Fig. 3).

If the sediment cores at station A are used as representative for the whole sub-reach A–B, the inventory in the sediment at the end of the exposure period ($t = +5.15$ h) can be determined. The inventory of chromium in the sediment constitutes ~93% of the loss found from the stream water BTCs. Hence, this implies that the predominant part of the chromium

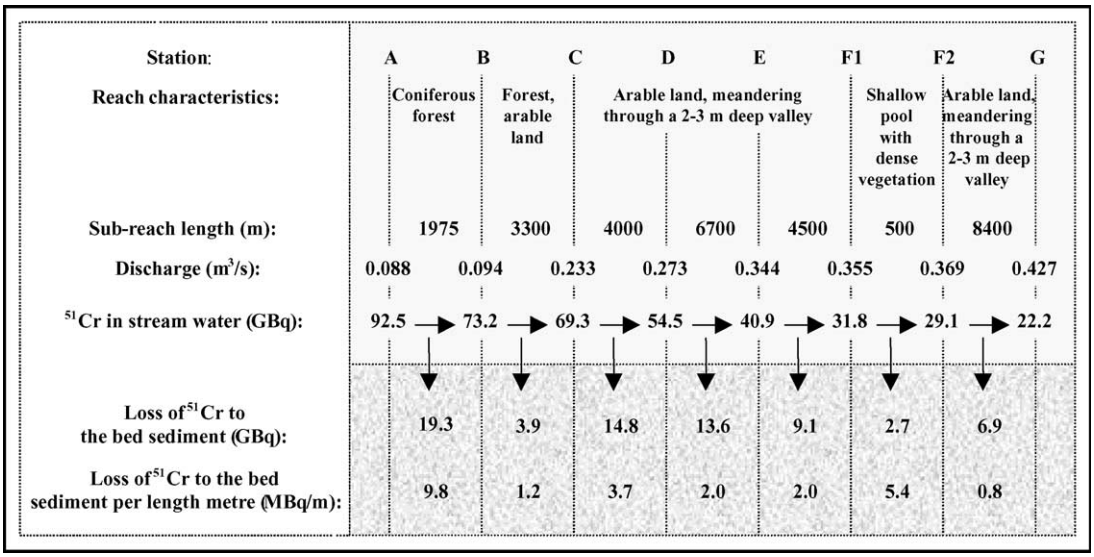

Fig. 2. Mass balance of chromium along the Säva Stream calculated by integrating the stream water BTCs to obtain the remaining mass in the stream water (and thereby the approximate loss to the sediment) directly after the passage of the pulse at each station (discharge determined by means of tritium data).

loss from the stream water occurs due to accumulation in the sediment.

By normalising the retained mass with the respective mass of the tracer in the uppermost layer ($z = 0–0.01$ m), the depth profiles of tritium and chromium can be compared (Fig. 4).

The profiles reveal that the main part of the tritium mass penetrates deeper into the sediment than the chromium tracer, which is retained due to adsorption on to sediment particles closer to the sediment surface.

The depth concentration profiles were also recalculated to BTCs of the mass inventory, where the tracer mass has been integrated down to a depth of 0.1 m (Figs. 5a and b and 6a and b).

To reveal if and how diagenetic processes influence the washout rate of chromium retained in the sediment, we used different extraction solvents on sub-samples of the sediment. Association of chromium with different substances with time could then be studied.

Differentiation into original given fraction classes (ion exchangeable, Fe and Mn oxides etc.) by Riise et al. (1990) and Broberg (1994) indicated in the right-hand column of Fig. 7 might be questioned for the Säva Stream Tracer Experiment due to

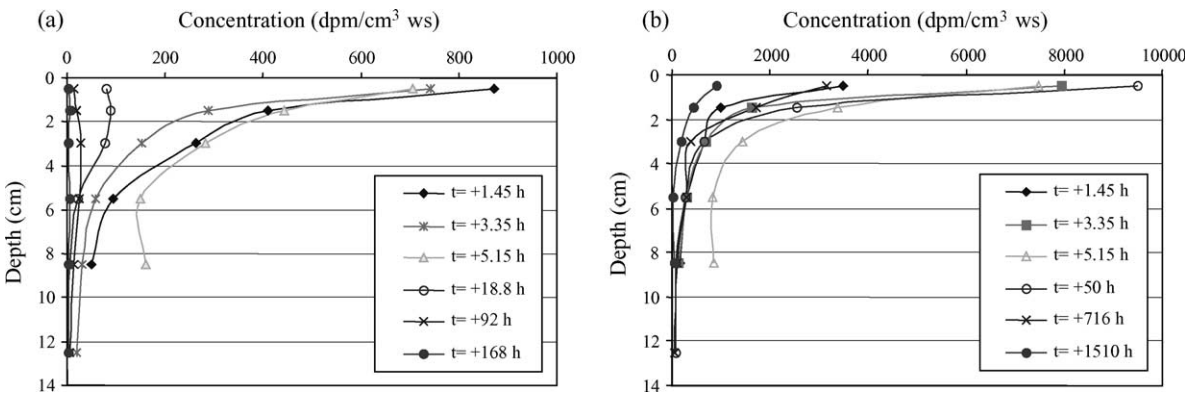

Fig. 3. Concentration profiles in the sediment versus depth at station A (a) tritium (b) chromium (ws denotes wet substance).

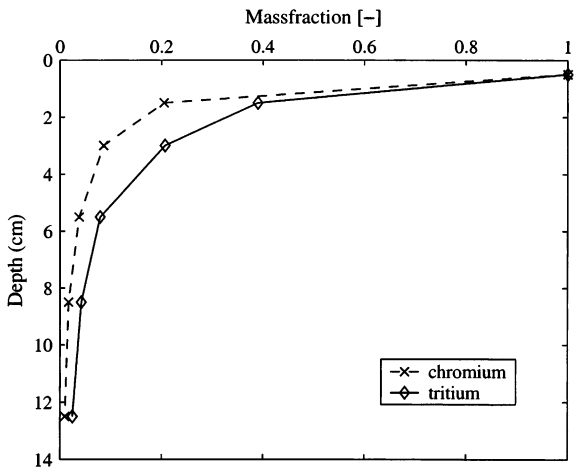

Fig. 4. Differences in the mass inventory profiles of chromium and tritium in the bed sediment at station A during the uptake phase ($t = +3.35$ h) of the two tracers.

the modified extraction scheme. However, the leaching procedure indicates that chromium mainly adsorbs on to substrate types as Fe and Mn oxides (adsorption and/or co-precipitation), humic matter (complexation and/or adsorption) and mineral constituents (adsorption). The results can also be used to indicate any change of the binding strength between chromium and the bed sediment that occurs over time. The results in Fig. 7 indicate that chromium becomes more strongly bound with time during washout from the sediment. This successive phase change of chromium sorption is consistent with the relatively slower and slower decay of the tail in the mass inventory BTCs (Figs. 5b and 6b).

In the absence of measured distribution coefficients for chromium in the sediment, K_B, we calculated an approximate range for the partitioning using the values of K_d and the particle concentration in the stream water and sediment. The K_B-value expresses the ratio between the adsorbed solute concentration (g_a [dpm/m^3 wet sediment]) and the dissolved solute concentration (g_d [dpm/m^3 wet sediment]). The transformation of K_d to K_B requires that we take into account changes in different environmental conditions between the water and the sediment such as particle concentration (dry weight per unit volume of medium), grain size, pH, redox potential, organic matter (LOI), etc. It was, however, not possible to account for all these environmental conditions. By considering only the effect of different particle concentrations in stream water (mean: 0.023 g dw/dm^3) and sediment (mean: 970 g dw/dm^3), a reference value of K_B was found to lie in the range 10,000–18,000. The same order of magnitude was also observed from measurements of the partition coefficient of Cr in the Vistula River, which was found to be equal to 20,000 (Brolin and Pettersson, 1998).

Samples from the sediment plate reveal a significant spatial variability of the concentration of adsorbed chromium within the sediment (Fig. 8).

Also the mass inventory BTCs in the sediment indicate a variability of the uptake in the sediment

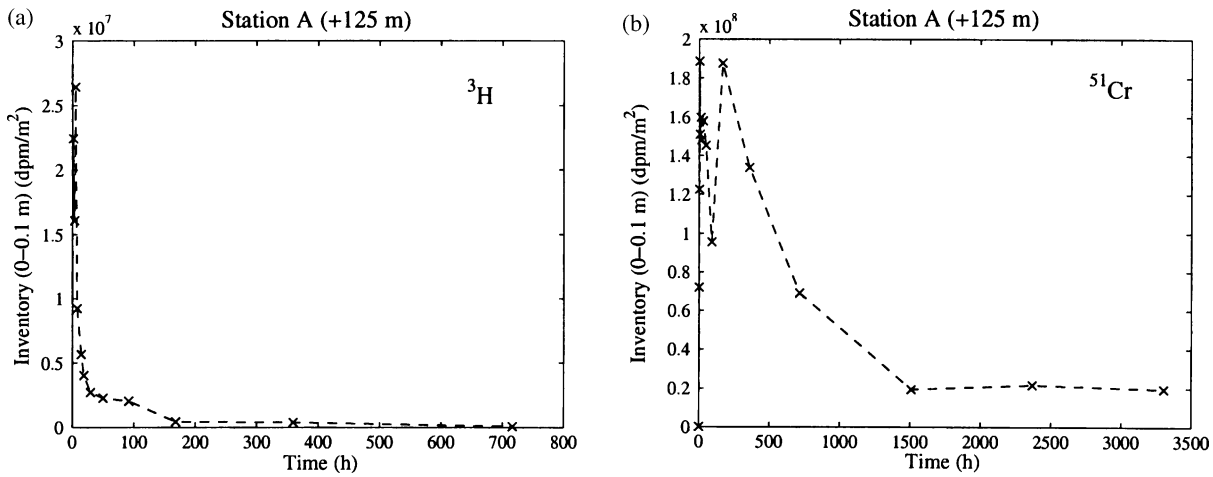

Fig. 5. Breakthrough curve of the mass inventory in the bed sediment (0–10 cm) at station A (a) tritium (b) chromium.

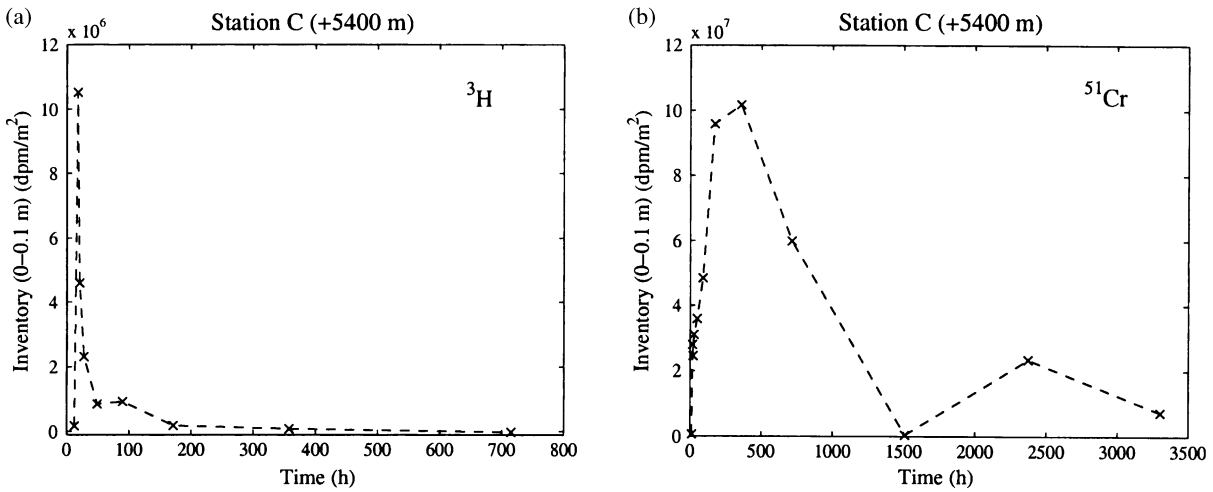

Fig. 6. Breakthrough curve of the mass inventory in the bed sediment (0–10 cm) at station C (a) tritium (b) chromium.

between different sampling occasions, especially for chromium at station A during the early uptake phase (Fig. 5b). The variability at different depth at $t = +3.35$ h, expressed as coefficient of variation, was determined by means of seven sediment cores to vary in the range 26–60% for tritium and 38–58% for chromium (Fig. 9). The corresponding coefficient of variation for the mass inventory (0–0.1 m) was determined to 23 and 36% for tritium and chromium, respectively.

The variability could be an effect of different sediment characteristics for the individual samples. A positive correlation was found between the organic content (= loss on ignition) or the water content in the sediment sample and the concentration of chromium (Fig. 10). There is a correlation between the water content and the loss on ignition. No dependence of the concentration of tritium in the sediment on the water content or the loss on ignition was found.

2.1.3. Additional stream characteristics

In addition to collecting water and sediment samples during the experiment, we measured geometrical dimensions of the stream at the sampling stations, slope and hydraulic conductivity. To get representative mean values of the geometrical dimension at the sub-reaches, we determined the hydraulic radius after the experiment at 70 locations along the stream. By comparing the size of the stream obtained at the sampling stations on the two occasions, we calculated representative mean values for the reaches

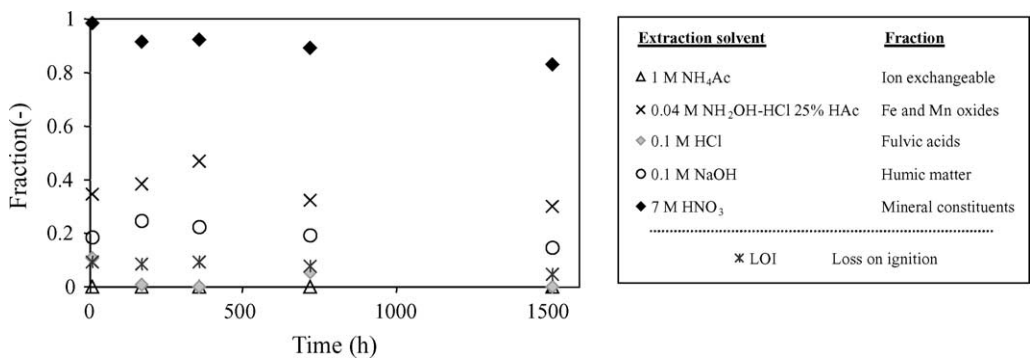

Fig. 7. Fractions of chromium extractable from the sediment at different instants of elapsed time after the completion of the injection at station A. The non-sequential extraction procedure used is a modified version of the extraction schemes by Riise et al. (1990) and Broberg (1994). The given fraction classes correspond to the original extraction scheme.

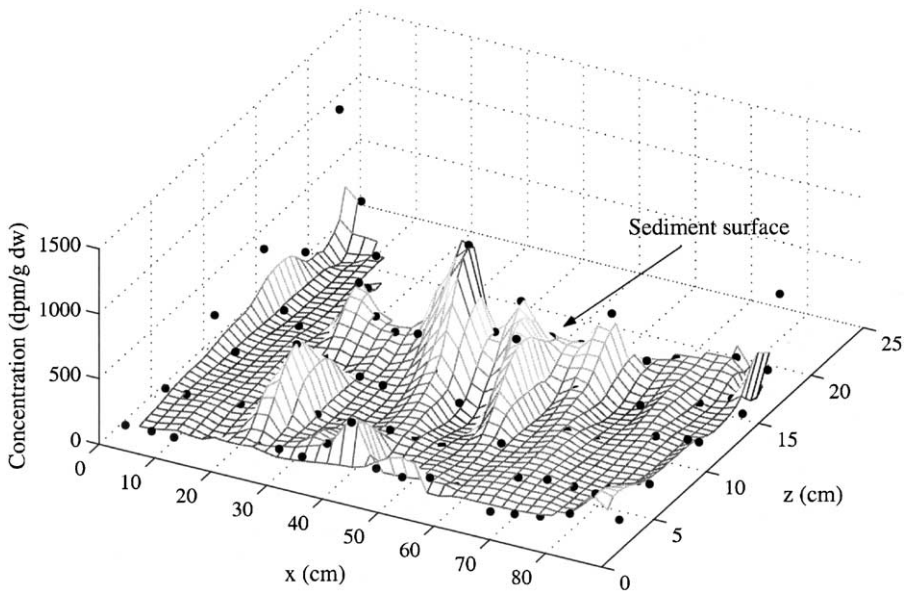

Fig. 8. Concentration of adsorbed chromium in a sediment plate expressed as activity per weight of dry substance. The plate was taken along the water stream direction x and with depth z approximately 20 h after the passage of the pulse at station A.

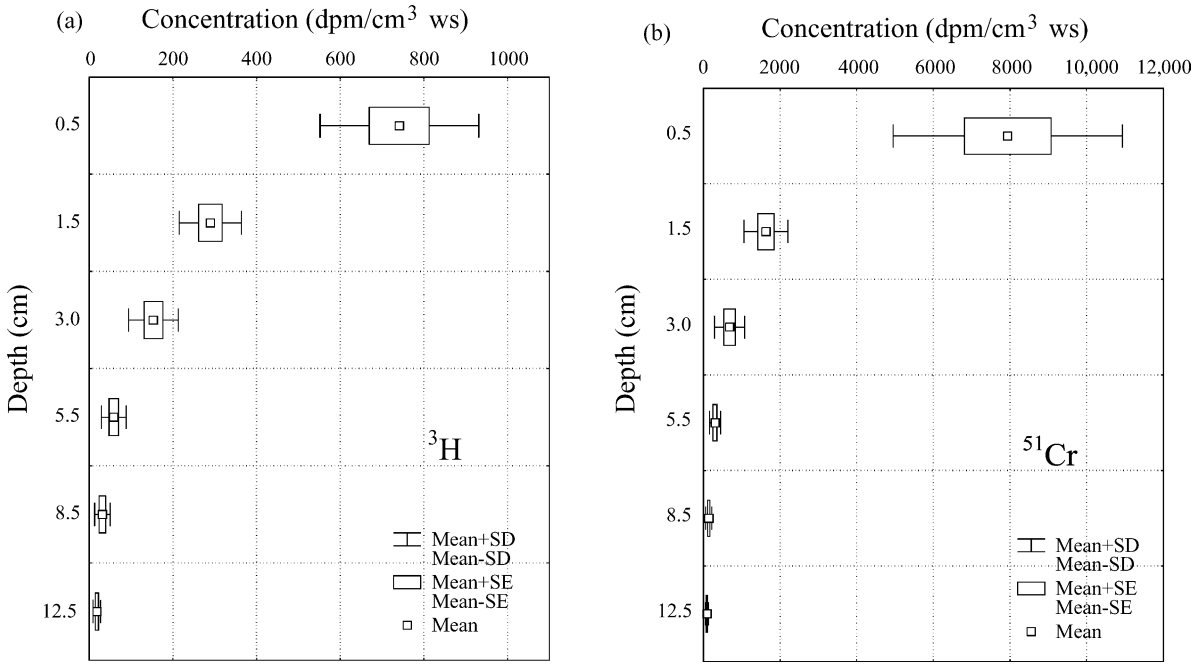

Fig. 9. Variability of the uptake of the tracers in the bed sediment at station A at $t = +3.35$ h (a) tritium (b) chromium. (SD = standard deviation, SE = standard error ($= \sqrt{SD^2/n}$), where n is the number of samples).

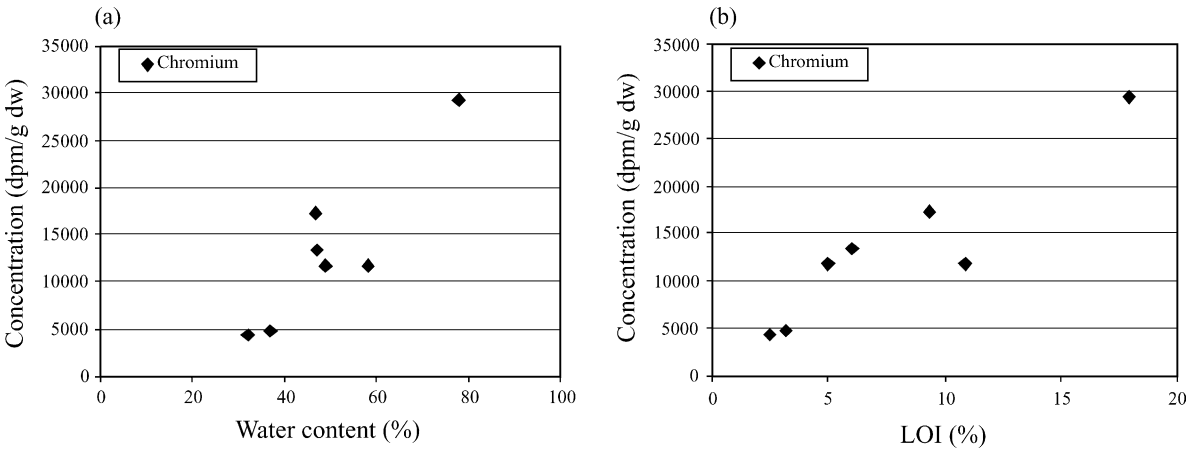

Fig. 10. Variability of the uptake of ^{51}Cr in the surficial layer (0–1 cm) of the bed sediment at station A at $t = +3.35$ h as a result of differences in the bed sediment characteristics (a) water content (b) loss on ignition (LOI).

(Table 1). Discharge was determined by dilution gauging technique using tritium data (Fig. 2).

3. Model

To evaluate the tracer experiment, we used a modelling concept similar to that of Jonsson and Wörman (2001). In this formulation the reactive substance chromium is assumed to exist in either dissolved or particulate form. The uptake of chromium on to particulate matter is assumed to be caused primarily by sorption. However, the formulation adopted here can also account for other uptake mechanisms such as precipitation and/or co-precipitation of chromium (including dissolution) with Fe and Mn hydroxides on to mineral grains. Since it would be difficult to determine which of these processes predominates, the uptake can be assumed to follow a single sorption isotherm. In order to explicitly account for precipitation/dissolution of Fe and Mn hydroxides during the sorption process, a formulation similar to the concept proposed by Runkel et al. (1999) could be used. In their model it is possible to account for the influence of pH on precipitation/dissolution and sorption.

A hypothesis in the present study is that the sorption on to particulate matter in the water phase equilibrate instantaneously, while the sorption in the sediment

Table 1
Parameter values along sub-reaches as obtained from model calibration to BTCs in the stream water

Measured parameters				Calibrated by means of ^{3}H		Calibrated by means of ^{51}Cr
Reach	Distance, Δx (m)	Hydraulic radius, h (m)	Flow dilution coefficient, ϕ (m^{-1})	Diffusion coefficient, D_s (m^2/s)	Effective flow velocity, u_e(m/s)	Sorption rate coefficient in bed sediment, k_2 (s^{-1})
A–B	1975	0.26	3.34×10^{-5}	5.0×10^{-9}	0.105	4.0×10^{-7}
B–C	3330	0.33	2.72×10^{-4}	2.0×10^{-8}	0.119	4.0×10^{-10}
C–D	4000	0.77	3.98×10^{-5}	2.0×10^{-7}	0.089	3.0×10^{-8}
D–E	6700	0.58	3.46×10^{-5}	8.0×10^{-8}	0.092	2.0×10^{-8}
E–F1	4500	0.90	6.94×10^{-6}	2.4×10^{-7}	0.076	1.8×10^{-8}
F1–F2	500	1.30	7.96×10^{-5}	4.0×10^{-6}	0.060	4.0×10^{-9}
F2–G	8400	0.97	1.73×10^{-5}	1.1×10^{-6}	0.070	4.2×10^{-9}

Parameters assumed constant: dispersion coefficient, $E = 0.8$ m^2/s, porosity, $\eta = 0.7$ [−], distribution coefficient in bed sediment, $K_B = 20,000$ [−].

phase is described as a kinetic first-order reaction. Several experiments have indicated that sorption of different substances on to particulate matter is kinetically controlled due to diffusion into the interior of grains (Nyffeler et al., 1984; Jannasch et al., 1988; Wörman et al., 1998). The reason for describing only the sorption in the sediment as a kinetic process is that larger particles are more common in the sediment than in the stream water and, hence, the inter-granular diffusion is more pronounced in the sediment. An experiment with Sr revealed that finer particles had a higher adsorbed solute concentration than coarser particles because of an instantaneous sorption equilibration with the finer particles and a slower sorption on to coarser particles (Bencala, 1983). In the stream water, the total available sites for adsorption are naturally also less numerous than in the bed sediment. Furthermore, a theoretical investigation by Jonsson and Wörman (2001) showed theoretically the relatively lower importance of considering the sorption kinetics in the stream water than in the bed sediment.

The exchange between the water and the bed sediment is assumed to be characterized as diffusive. This assumption is supported by laboratory experiments by Elliott and Brooks (1997a,b), field observations of Wörman et al. (1998) and observations in the present study (Fig. 3a).

The porosity in the bed sediment is assumed to be constant with depth.

Based on the above simplifications, the transport equation in the main stream is stated as:

$$\frac{\partial c_T}{\partial t} + \frac{1}{A(x)(1+K_R)}\left(c_T\frac{\partial Q(x)}{\partial x} + Q(x)\frac{\partial c_T}{\partial x}\right) - \frac{1}{A(x)(1+K_R)}\frac{\partial}{\partial x}\left(A(x)E\frac{\partial c_T}{\partial x}\right) = \frac{P(x)}{A(x)}\eta D_s\left.\frac{\partial g_d/\eta}{\partial z}\right|_{z=0} \quad (1)$$

where c_T is the total solute mass in the stream water per unit volume of water (kg/m^3), g_d the dissolved solute mass in the bed sediment per unit volume of wet sediment (including pores and solids) (kg/m^3), t the time (s), $A(x)$ the cross-sectional area of the main stream (m^2), K_R the ratio of the cross-sectional area of the sidepockets and the cross-sectional area of the main stream [−] (Wörman et al., 1998), $Q(x)$ the discharge in the stream ($Q(x) = vA(x)$) (m^3/s), E the longitudinal dispersion coefficient (m^2/s), D_s the exchange diffusion coefficient in the pore water (m^2/s), η the porosity in the bed sediment [−], x the longitudinal co-ordinate (m), z the lateral co-ordinate (m) and $P(x)$ the wetted perimeter of the stream (m).

The partition ratio at equilibrium of adsorbed solute mass per unit volume of water, c_a (kg/m^3), and the dissolved solute mass per unit volume of water, c_d (kg/m^3), is defined by the distribution coefficient, $K_d = [c_a/c_d]$ [−].

The mass conservation equations representing the vertical transport in the sediment are:

$$\frac{\partial g_d}{\partial t} - D_s\frac{\partial^2 g_d}{\partial z^2} + k_2(K_B g_d - g_a) = 0 \quad (2)$$

$$\frac{\partial g_a}{\partial t} - k_2(K_B g_d - g_a) = 0 \quad (3)$$

where g_a is the adsorbed solute mass in the bed sediment per unit volume of wet sediment (including pores and solids) (kg/m^3), k_2 the sorption rate coefficient in the bed sediment (s^{-1}) and K_B the equilibrium distribution coefficient in the bed sediment ($K_B = [g_a/g_d]_{eq}$).

3.1. Solution of equations

The dominating processes can be evaluated by interpretation of the breakthrough curves in both stream water and bed sediment. In this section we present the solutions to the BTCs.

3.1.1. Solution for breakthrough curves in the stream water

The system of equations (Eqs. (1)–(3)) is solved for a unit Dirac pulse by means of Laplace transforms. The boundary conditions are given by:

$$c_T(x = 0, t \geq 0) = \frac{M}{Q_0}\delta(t = 0) \quad (4)$$

$$c_T(x = \infty, t \geq 0) = 0 \quad (5)$$

$$g_d(z = \infty, t \geq 0) = 0 \quad (6)$$

$$g_d(z = 0, t \geq 0) = \eta\, c_d(x, t \geq 0) \quad (7)$$

where M is the total amount of solute introduced in the system (kg) Q_0 the discharge at the upper boundary (m^3/s) and $\delta(t)$ is Dirac's delta function (s^{-1}).

The initial conditions are given by:

$$c_T(x > 0, t = 0) = g_d(z, t = 0) = g_a(z, t = 0) = 0 \quad (8)$$

On the assumption that

$$\frac{\partial AE}{\partial x}\frac{\partial c_T}{\partial x} \ll AE\frac{\partial^2 c_T}{\partial x^2}$$

the equation to be solved can be stated in the Laplace domain as:

$$\frac{\partial^2 \bar{c}_T}{\partial x^2} - \frac{u_e}{E}\frac{\partial \bar{c}_T}{\partial x} - \left(p + \frac{D_s \eta}{(1+K_d)h}\sqrt{\frac{p\left(1 + K_B\frac{k_2}{p+k_2}\right)}{D_s}} + u_e\frac{\frac{\partial Q}{\partial x}}{Q}\right)\frac{\bar{c}_T}{E} = 0 \quad (9)$$

The discharge variation along the sub-reaches was assumed to fulfil the condition $(1/Q)\partial Q/\partial x =$ constant. This condition is fulfilled when the discharge increases exponential along the sub-reaches as $Q = Q_0\, e^{\phi x}$, where x is the distance (m) and ϕ a flow dilution coefficient (m^{-1}). A reason for assuming the exponentially varying discharge with distance is that a solution can be found in closed form in the Laplace domain. The solution here is:

$$\bar{c}_T = \frac{M}{Q_0}\exp\left[\left(\frac{u_e}{2E} - \sqrt{\frac{u_e^2}{4E^2} + \frac{p}{E} + \frac{D_s\eta}{E(1+K_d)h}\sqrt{\frac{p\left(1+K_B\frac{k_2}{p+k_2}\right)}{D_s}} + \frac{u_e\phi}{E}}\right)x\right] \quad (10)$$

where $u_e = v/(1+K_R)$ (m/s), p the Laplace operator and h is the hydraulic radius ($h = A(x)/P(x)$) (m).

However, if dispersion is negligible ($E = 0$), it is easily verified that the effect of dilution appears as a scaling factor in front of the solution to the problem without any dilution, both for the exponentially varying flow given above but also for a linearly increasing flow (Eq. (11)).

For the exponentially varying flow, the scaling factor, ψ will take the form $e^{-\phi x}$. For a flow increasing linearly with distance, $Q = Q_0(1+\alpha x)$, Forsman (2000) showed that the corresponding scaling factor introduced in this case can be expressed as $1/(1+\alpha x)$.

For sufficiently small values of the dispersion coefficient, the main effect of dilution is therefore a scaling of the concentrations and, thus, the exact discharge variation is not essential.

To obtain numerical inversion of Eq. (10) (i.e. BTCs) we used a numerical algorithm by De Hoog et al. (1982) implemented by Hollenbeck (1998). Convolution is used to get the solution for a concentration pulse of finite duration and varying magnitude.

3.1.2. Solution for breakthrough curves in the bed sediment

To be able to fit the model to the sediment BTCs, we combine Eqs. (2) and (3) with the boundary conditions Eqs. (6) and (7). The equations to be solved can be stated in the Laplace domain as:

$$\bar{c}_T = \underbrace{\psi}_{\text{scaling factor}}\ \underbrace{\frac{M}{Q_0}\exp\left[-\left(\frac{p}{u_e} + \frac{D_s\eta}{u_e(1+K_d)h}\sqrt{\frac{p\left(1+K_B\frac{k_2}{p+k_2}\right)}{D_s}}\right)x\right]}_{\text{solution to problem without dilution}} \quad (11)$$

$$p\bar{g}_d - D_s \frac{\partial^2 \bar{g}_d}{\partial z^2} + k_1(K_B\bar{g}_d - \bar{g}_a) = 0 \quad (12)$$

$$p\bar{g}_a - k_1(K_B\bar{g}_d - \bar{g}_a) = 0 \quad (13)$$

The resulting expression of the total concentration in the sediment, $g_{tot}(= g_d + g_a)$, in the Laplace domain is:

$$\bar{g}_{tot} = \left(1 + \frac{K_B k_2}{p + k_2}\right)\bar{c}_d(x, z = 0)\eta\, \mathrm{e}^{-\sqrt{(\theta/D_s)}z} \quad (14)$$

where

$$\theta = p + k_2 K_B - \frac{K_B k_2^2}{p + k_2} \text{ and } p \text{ is the Laplace operator.}$$

Integration of Eq. (14) to a certain depth, z_{int}, gives the Laplace transform of the total inventory of solute mass down to the depth z_{int} per unit bed area (kg/m^2), when a unit pulse is introduced at the boundary between time t_1 and t_2 :

$$\bar{M}_{tot} = \int_0^{z_{int}} \bar{g}_{tot}\mathrm{d}z = \left(1 + \frac{K_B k_2}{p + k_2}\right)\frac{\eta \bar{c}_T}{K_d + 1} \times \sqrt{\frac{D_s}{\theta}}\left(1 - \mathrm{e}^{-\sqrt{(\theta/D_s)}z_{int}}\right)\left(\frac{\mathrm{e}^{-t_1 p} - \mathrm{e}^{-t_2 p}}{p}\right) \quad (15)$$

where

$$\theta = p + k_2 K_B - \frac{K_B k_2^2}{p + k_2}.$$

The numerical algorithm by De Hoog et al. (1982) and the code of Hollenbeck (1998) are used to get the real-domain solution of Eq. (15). Superposition of the real-domain solutions of Eq. (15) for all the pulses that constitute the boundary condition gives the total amount of tracer in the sediment for a variable concentration in the stream water.

4. Model evaluation

4.1. Evaluation by means of stream water data

By means of the real domain solution of Eq. (10), the model was fitted 'by eye' to the observed BTCs in the stream water. The fitting was performed at sub-reaches along the stream with the observed BTC at one station as a boundary condition for the next one. The conservative properties of the transport, the stream hydraulics, were first evaluated by means of the tritium BTCs at the eight stations. These properties were then held constant when the sorption characteristics were evaluated by means of the chromium BTCs. A few parameters were measured independently in the field, while others were assigned plausible values based on literature information (see Table 1). The value of the porosity used in the model is constant with depth and based on the porosity in the uppermost 2 cm of the sediment samples.

Because of the inherent subjectivity of the 'by eye' evaluation it does not yield a unique result in terms of values of the included parameters. This problem is remedied to some degree by using observations independent of the tracer BTCs.

The magnitude of the dispersion coefficient is based on determinations of the dispersion coefficients by the authors in streams with similar geometry, and also on an approximate recalculation of the dispersion coefficients reported in literature. Using the Elder relationship (Fischer et al., 1979), which states that the dispersion coefficient is proportional to the water depth and shear velocity, the dispersion coefficients reported by Bencala and Walters (1983) was rescaled and found to be approximately 0.8 m^2/s. As a variation of the dispersion coefficient around this value seemed to have negligible influence on the solution, it was assumed constant.

For a dispersion coefficient of this magnitude, it was also found that Eqs. (10) and (11) yielded similar results in the evaluation of the exchange parameters and the exact representation of the flow was therefore not essential.

During the evaluation of the sorption rate coefficient by means of the stream water BTCs, the K_B-value is held constant at 20,000 and the K_d at 0.3 (Section 2.1). Table 1 lists the parameter values obtained from the fit at the different sections.

As can be seen in Figs. 11 and 12, where the observed and fitted BTCs are shown, there is an acceptable representation of the processes affecting the tritium transport in the stream. The fact that the model nicely fits also the tails of the breakthrough indicates that the exchange with the surrounding hyporheic zone can be described using the diffusive formulation.

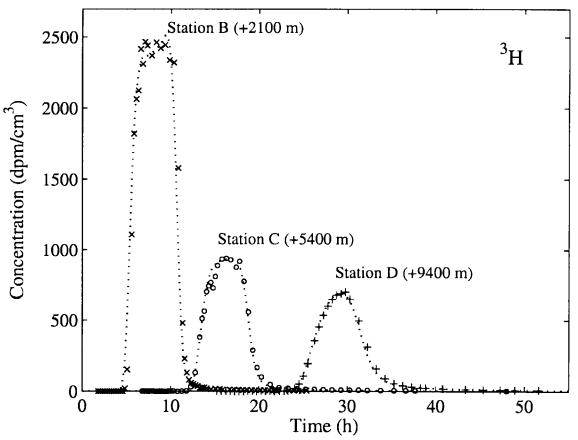

Fig. 11. Observed and simulated BTCs of tritium in the stream water at stations B–D.

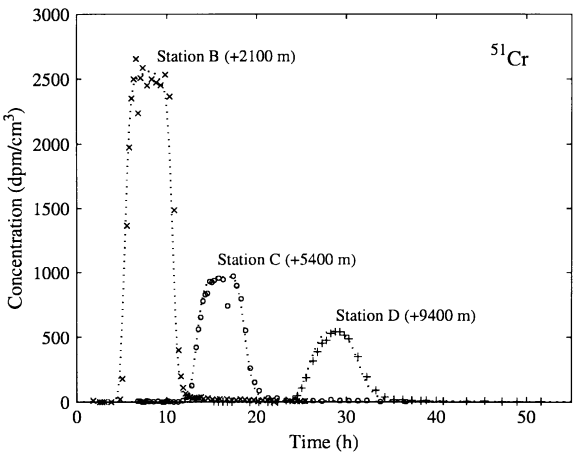

Fig. 13. Observed and simulated BTCs of chromium in the stream water at stations B–D ($K_B = 20,000$).

The investigated range of the parameters can be expressed in the dimensionless numbers xu_e/D_s, x/h and xu_e/E. The first two numbers were calculated reach-wise and summed to obtain characteristic values for the total investigated reach. The dispersion coefficient was not determined with a high degree of accuracy and was not included in the following comparison. Hence, the maximum parameter values covered in this study were $x/h = 4.9 \times 10^4$ and $xu_e/D_s = 7.3 \times 10^{10}$.

To make a comparison with results from previous tracer tests, an approximate recalculation of their results were made to find the investigated ranges of xu_e/D_s and x/h. A conclusion is that the present study comprised a wider range in terms of xu_e/D_s and x/h than most previous reported tracer studies (Bencala and Walters, 1983; Harvey and Fuller, 1998; Wörman, 1998). An incomplete reporting of exact flow conditions in many studies makes it, however, impossible to calculate and compare all dimensionless relevant parameters.

The model could also be fitted to the BTCs of chromium (Figs. 13 and 14). However, the fit is not as good as for tritium. This is partly due to the fact that

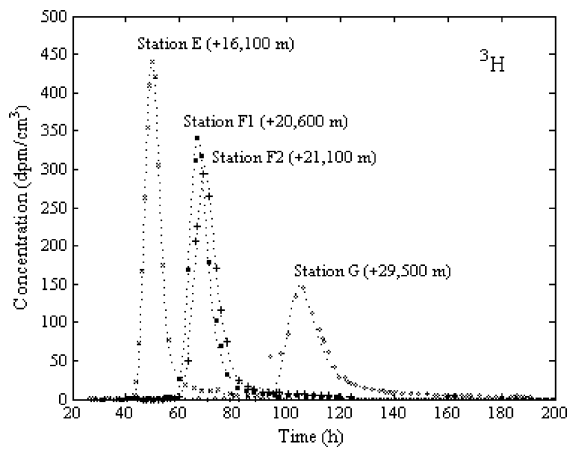

Fig. 12. Observed and simulated BTCs of tritium in the stream water at stations E–G.

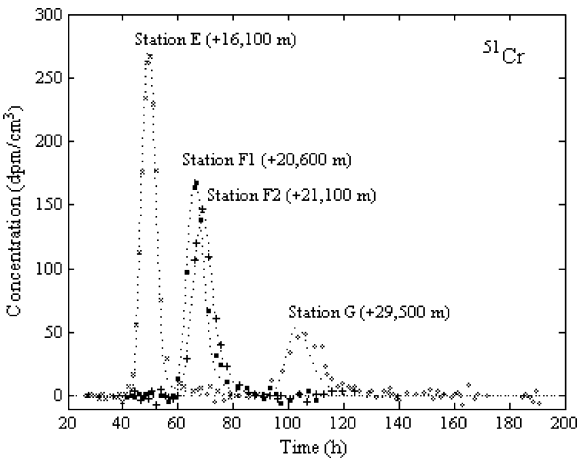

Fig. 14. Observed and simulated BTCs of chromium in the stream water at stations E–G ($K_B = 20,000$).

the quality of the chromium data is poorer than that of the tritium data.

We also tested the model under the assumption of instantaneous sorption ($k_2 = \infty$). In this case, the distribution coefficient, K_B, was the only parameter that was calibrated against the chromium water BTCs. A K_B-value equal to 15 gave the best fit with respect to peak value of the BTC. However, we can conclude that the instantaneous sorption model was not acceptable since such a description produces too high concentrations in the tails of the BTCs and a clear retardation of the propagation velocity shown as a timelag of the peak (Fig. 15).

4.2. Evaluation by means of sediment data

By means of the real-domain solution to Eq. (15), it was also possible to make an independent fit 'by eye' of the model to the BTCs in the bed sediment by adjusting the diffusion coefficient, D_s. The porosity value was the same as for the fit to the water BTCs. The results from the fit to the observed inventory of tritium in the uppermost 10 cm of the sediment at stations A and C are given in Figs. 16 and 17, respectively.

Due to the high temporal variability of the uptake of chromium, especially during the early uptake phase, the fit was not as good for chromium as for tritium

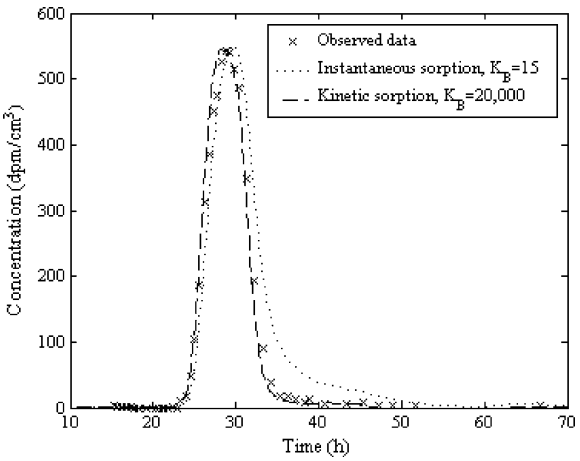

Fig. 15. Comparison of simulated chromium BTCs with observed chromium BTC at station D, with a kinetic sorption ($K_B = 20,000$ and $k_2 = 3 \times 10^{-8}$ s^{-1}) and an instantaneous sorption concept ($K_B = 15$, $k_2 = \infty$), respectively.

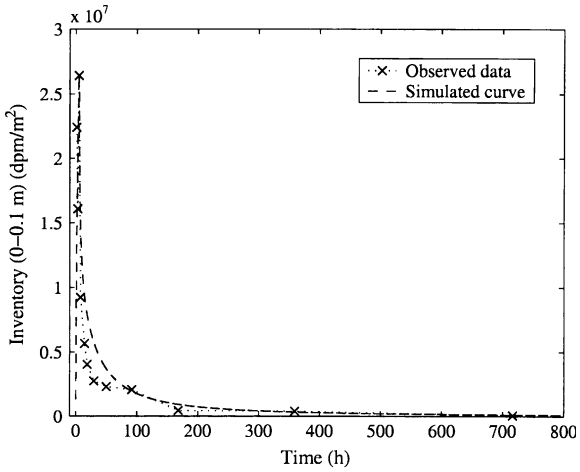

Fig. 16. Model solution fitted to the observed inventory of tritium in the uppermost 10 cm of the sediment at station A ($D_s = 9 \times 10^{-9}$ m^2/s).

(Fig. 18). As can be seen in Fig. 8, the early solute uptake of chromium in the sediment seems to be distributed predominantly along certain verticals. With time, longitudinal groundwater movements are likely to smooth out these differences and provide more reliable data. Consequently, the scatter of the data around the model is decreasing with time in Fig. 18.

Fig. 18 also suggests the need for a kinetic sorption in the bed sediment since an instantaneous

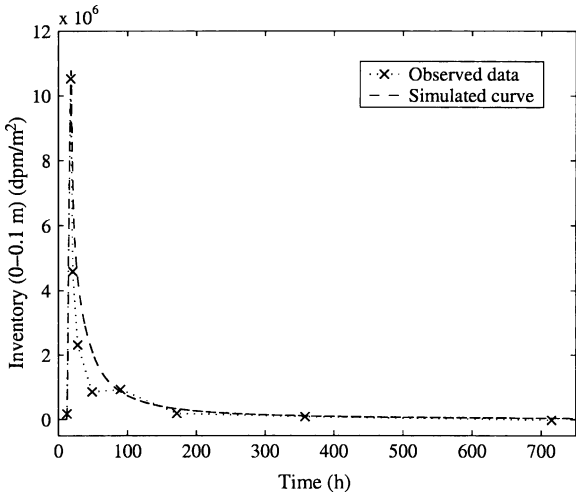

Fig. 17. Model solution fitted to observed inventory of tritium in the uppermost 10 cm of the sediment at station C ($D_s = 1.4 \times 10^{-8}$ m^2/s).

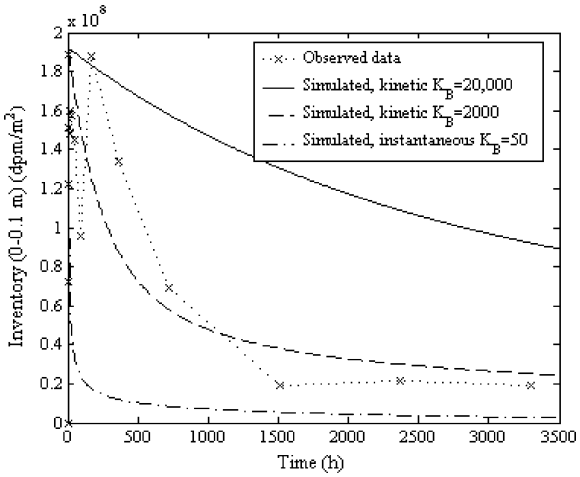

Fig. 18. Model solutions fitted to the observed inventory of chromium in the uppermost 10 cm of the sediment at station A. Simulation results represent fits with an instantaneous sorption concept ($D_s = 9 \times 10^{-9}$ m^2/s, $K_B = 50$, $k_2 = \infty$) and a kinetic sorption concept ($D_s = 9 \times 10^{-9}$ m^2/s, $K_B = 20,000$, $k_2 = 1.6 \times 10^{-7}$ s^{-1} and $D_s = 9 \times 10^{-9}$ m^2/s, $K_B = 2000$, $k_2 = 1.6 \times 10^{-6}$ s^{-1}).

description of sorption ($k_2 = \infty$) yielded an insufficient fit to the chromium mass inventory BTCs. The best fit with respect to peak value for the instantaneous sorption model was obtained for $K_B = 50$. However, although the peak values were matched, instantaneous sorption produced a washout that was much faster than the observed (Fig. 18).

A kinetic sorption model description with $K_B = 20,000$, consistent with the recalculated K_d that gave an acceptable fit to the stream water BTCs, yielded a predicted washout of chromium that was much slower than the observed, provided that the peak-values were matched (Fig. 18). Adjusting the K_B-value to 2000 gave a simulated curve that described the observed washout much better (Fig. 18).

4.3. Comparison of evaluation results from the independent tracer observations in the stream water and bed sediment

The model calibrations using both the water and the sediment tritium BTCs indicate that the diffusive concept can be used to characterize the solute exchange with the hyporheic zone. The magnitude of the exchange is quantified with the lumped parameter D_s. At stations A and C, where sediment samples were taken, it is possible to compare the value of D_s obtained from the fit to the water BTC with that obtained from the fit to the sediment BTC. The values are not exactly the same, but are still of the same order of magnitude (Station A: D_s(water)/D_s(sediment) = 0.6; Station C: D_s(water)/D_s(sediment) = 1.4). The deviation between these results is reasonable, especially in the light of the fact that we compare a point observation with a high variability, with the integrated result along an entire reach between measuring stations. This implies that sediment sampling is not necessary for evaluating the diffusive exchange, but rather, that it can be evaluated from stream water BTCs alone.

Unlike the evaluation of the hydraulic exchange properties, in which the results from the stream water and sediment were similar, the evaluation of the sorption characteristics depended on type of observation. The need for a kinetic description of the chromium sorption was, however, evident from the fit of the model both to the stream water and sediment BTCs (Figs. 15 and 18).

The value on K_B based on the recalculated K_d ($K_B = 20,000$), provided a correct description of the observations in the water but not of the washout from the sediment. The K_B-value that described the washout from the sediment best ($K_B = 2000$) was then used to test the resulting fit to the stream water BTCs. As can be seen in Figs. 19 and 20, the simulated curves follow the observed once also for this K_B-value. Hence, to make a certain statement about the sorption characteristics i.e. to reduce the range of K_B, tracer observations in the sediment are needed. A consistent result in terms of interpretation of chromium concentration in the sediment and in the water was obtained for $K_B = 2000$.

Table 2 lists the resulting values of the sorption rate coefficient from the model calibration at the different sub-reaches.

The value of the sorption rate coefficient, assuming $K_B = 2000$, from the fit of the model to the stream water BTC at sub-reach A–B was 4×10^{-6} s^{-1} compared with 1.6×10^{-6} s^{-1}

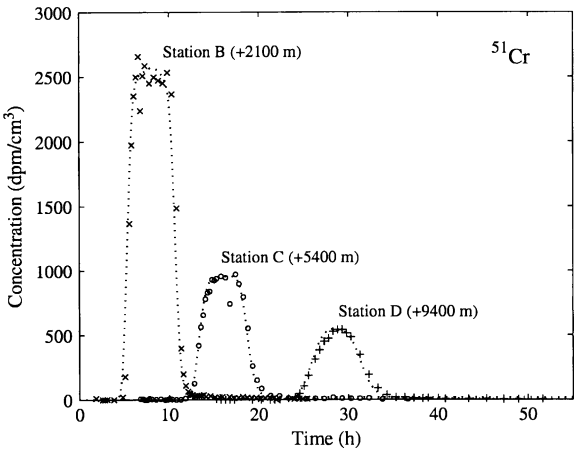

Fig. 19. Observed and simulated BTCs of chromium in the stream water at stations B–D ($K_B = 2000$).

obtained from an independent calibration against the sediment BTC. Part of the deviation could be attributed to the fact that different values of the diffusion coefficient have been used when fitting to the water and sediment, respectively (Water: $D_s = 5 \times 10^{-9}$ m^2/s; Sediment: $D_s = 9 \times 10^{-9}$ m^2/s). Even though it is difficult to determine exactly the rate coefficient from the performed experiment, the evaluations of the sediment and the water still indicate the same order of magnitude of the rate coefficient. At least the need for a rate-limited description of sorption on to particulate matter in the bed sediment is apparent.

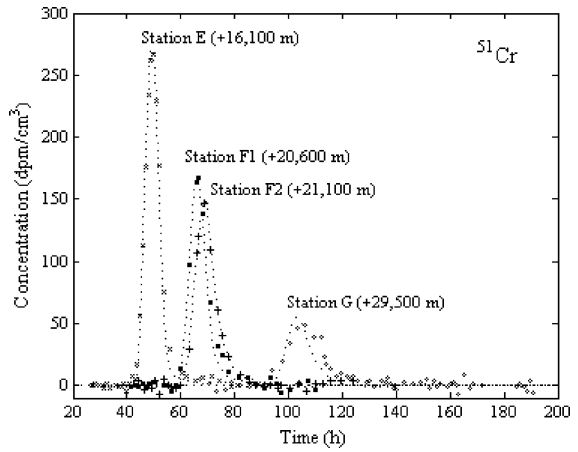

Fig. 20. Observed and simulated BTCs of chromium in the stream water at stations E–G ($K_B = 2000$).

Table 2
Sorption rate coefficients obtained from model calibration versus stream water BTCs, when the equilibrium distribution coefficient, K_B, equals 2000. Additional parameters used in the simulations are those given in Table 1

Sub-reach	Sorption rate coefficient, k_2 (s^{-1})
A–B	4×10^{-6}
B–C	2×10^{-8}
C–D	3×10^{-7}
D–E	2×10^{-7}
E–F1	2.1×10^{-7}
F1–F2	2×10^{-8}
F2–G	4×10^{-8}

5. Discussion

The type and amount of data with which the transient storage model is calibrated significantly affect the precision of the parameter values. In this study, a simultaneous injection of both a conservative and a reactive substance facilitated an evaluation of both hydraulic and sorption properties.

The observations of solute concentration in both water and sediment reveal significant differences in the transport of the two substances. Specifically, chromium is subject to a marked retardation due to exchange with the hyporheic zone and sorption on to particulate matter in the sediment. The washout time representing a 75% decrease of the maximum uptake in the sediment is ~85 times longer for chromium than for tritium at station A (i.e. ~45 days) (Fig. 5a and b). Results of the extraction procedure indicate that the substrates on to which chromium is mainly adsorbed are Fe and Mn oxides, humic matter and mineral constituents.

From the BTCs in the sediment and also from the analyses of the sediment plate taken during the experiment, it is clear that a rather high spatial variability of chromium concentration prevails in the sediment especially during the early uptake phase (Figs. 5b and 8). The variability is probably partly caused by preferential flow paths that form in the sediment due to higher hydraulic conductivity in some zones leading to a higher adsorbed concentration in those areas (Fig. 8). With time, it

is likely that longitudinal groundwater movements smooth out these local concentration differences. Irregularities on the sediment surface can also induce different pressure heads at different locations and thereby cause different uptake rates in the resulting inflow and outflow areas. We also noted that part of the chromium uptake variability in the sediment was correlated to differences in the water content and organic carbon (LOI) in the sediment (Fig. 10).

Results of the model calibrations indicate that sampling of either water or sediment is sufficient to determine the hydraulic properties. It was found possible to represent the exchange of a conservative substance between the water and the sediment with a diffusive flux formulation. The magnitude of the exchange is quantified with a lumped diffusion coefficient, D_s. Evaluation by means of the tritium stream water BTCs yielded D_s-values for the different sub-reaches in the range 5×10^{-9}–4×10^{-6} m^2/s with a coefficient of variation of 181% along the whole reach.

The evaluation of the diffusion coefficient at station A using the tritium inventory in the bed sediment yielded values of the same order of magnitude as the evaluation using the stream water BTC at sub-reach A–B (Water: $D_s = 5 \times 10^{-9}$ m^2/s; Sediment: $D_s = 9 \times 10^{-9}$ m^2/s). Therefore, observations of the concentration in the sediment are not crucial to the evaluation of the magnitude of the hydraulic properties, but rather these can be evaluated from stream water BTCs alone.

Our results further indicate that chromium is sorbed kinetically. This conclusion could be drawn from fitting the model to chromium concentration in either the sediment or in the flowing water (Figs. 15 and 18). However, if the sorption parameters are to be quantified with an acceptable degree of accuracy, we need data of the chromium concentration in the sediment. The reason for this is that the time scale reflected in the sediment data is sufficiently long to capture the relatively slow change in the sorption state and the washout of chromium from the hyporheic zone.

The proposed model with a first-order sorption formulation could acceptably describe the chromium observations in both stream water and bed sediment. If only the chromium BTCs in the stream water were to evaluate the model, the equilibrium distribution coefficient in the sediment could be varied in a wide range (covering several orders of magnitude) with an acceptable fit. The range in K_B based on the recalculation of the stream water K_d and the measured K_B-value for the Vistula River was determined to 10,000–20,000. This range falls within that producing an acceptable fit to the stream water BTCs.

An independent evaluation of the sorption process versus the observations of chromium in the bed sediment yielded, however, a much more narrow range of K_B, i.e. the uncertainty could be decreased. The 'best fit' to the sediment BTC at station A yielded a K_B-value around 2000 with a fairly small variation (Fig. 18). This value could also be used to produce an acceptable representation of the stream water BTCs. Due to the high variability in the uptake of chromium in the sediment, it is, however, possible that another type of kinetic description can also be appropriate. Independent observations of the distribution coefficient in the sediment could improve the possibility to differentiate different sorption isotherms.

The time scales of the sorption process (i.e. k_2^{-1}) obtained from assuming either $K_B = 20,000$ or $K_B = 2000$ (and a model fitting), differ by a factor of ~ 10 (Table 3). A K_B-value equal to 20,000 associates with a time scale of the sorption of 28.9 days, which is not consistent with the fact that the stream water BTC against which the calibration is made does not last longer than 2 days. The breakthrough curves in the sediment last over a time period of several months, which adequately captures the time scales of the sorption process.

Table 3
Time scales of sorption expressed as the inverse of the sorption rate coefficient given by the different model calibrations at sub-reach A–B to sediment and water BTCs, respectively

Data	K_B [−]	k_2 (s^{-1})	$1/k_2$ (days)
Sediment BTC	2000	1.6×10^{-6}	7.2
Water BTC	20,000	4×10^{-7}	28.9
Water BTC	2000	4×10^{-6}	2.9

6. Conclusions

A simultaneous injection of ^{3}H and $^{51}Cr(III)$ gave us the opportunity to reveal the difference of the transport characteristics between a conservative and a reactive solute in the Säva Stream.

Chromium is markedly retained in the bed sediment due to exchange with the hyporheic zone and sorption, while the washout of tritium is much faster. We found that tritium penetrated deeper in the sediment, whereas chromium to a greater extent was accumulated due to sorption in the uppermost part of the sediment. The loss of chromium mass from the stream water along the 30 km study reach, relative to tritium, was found to be 76% directly after the passage of the pulse in the stream water. The bed sediment hosted the main part of this loss. With time the chromium was slowly washed out from the sediment with a detectable rate during 5 months. Results from an extraction procedure showed that the chromium fraction remaining in the sediment was more strongly attached to the sediment with time due to a successive change in the binding characteristics.

The exchange between the sediment and the water was found to follow fairly well a diffusive flux formulation. The diffusion coefficient can be evaluated from either water or sediment BTCs.

A rate-limited sorption of chromium on to the sediment particles was observed from studying the chromium concentration both in the flowing stream water and in the sediment. Exclusion of the rate-limited sorption produced too low a concentration in the tails of the BTCs in the sediment. To quantify the time scales of sorption, it is crucial to utilise data of the long-term change of the solute concentration in the bed sediment, which captures the washout of the tracer. Generally, the time scales for sorption processes are not accurately captured in the solute concentration in the water. Using sorption parameters evaluated from stream water BTCs alone can therefore result in an unsatisfactory interpretation of the washout rate of reactive substances.

This study indicates that a satisfactory representation of the transport of reactive substances in streams requires consideration of sorption kinetics in the interpretative model.

Acknowledgements

The authors would like to thank their colleagues at the Department of Earth Sciences, Sedimentology for sampling assistance during the field experiment. The financial support of The Swedish National Energy Administration is gratefully acknowledged. Thanks are due to Bernhard H. Schmid and one anonymous reviewer for their comments in connection with their review for Journal of Hydrology.

References

Bencala, K.E., 1983. Simulation of solute transport in a mountain pool-and-riffle stream with a kinetic mass transfer model for sorption. Water Resour. Res. 19 (3), 732–738.

Bencala, K.E., Walters, R.A., 1983. Simulation of solute transport in a mountain pool-and-riffle stream: a transient storage model. Water Resour. Res. 19 (3), 718–724.

Bencala, K.E., McKnight, D.M., Zellweger, G.W., 1990. Characterization of transport in an acidic and metal-rich mountain stream based on a lithium tracer injection and simulations of transient storage. Water Resour. Res. 26 (5), 989–1000.

Broberg, A., 1994. The distribution and characterization of ^{137}Cs in lake sediments. In: Dahlgaard, H., (Ed.), Nordic Radioecology; The Transfer of Radionuclides through Nordic Ecosystem to Man, Elsevier, Amsterdam.

Brolin, A., Pettersson, A., 1998 Distribution of metals in sediment and water of the upper reaches of the Vistula River, Poland. M.Sc Thesis work. Institute of Earth Sciences, Uppsala University, Sweden. ISSN 1401-5765.

Chapra, S.C., Wilcock, R.J., 2000. Transient storage and gas transfer in lowland stream. J. Environ. Eng. 126 (8), 708–712.

De Hoog, F.R., Knight, J.H., Stokes, A.N., 1982. An improved method for numerical inversion of Laplace transforms. J. Sci. Stat. Comput. 3, 357–366.

Elliott, A.H., Brooks, N.H., 1997a. Transfer of nonsorbing solutes to a streambed with bed forms: theory. Water Resour. Res. 33 (1), 123–136.

Elliott, A.H., Brooks, N.H., 1997b. Transfer of nonsorbing solutes to a streambed with bed forms: laboratory experiments. Water Resour. Res. 33 (1), 137–151.

Fischer, H.B., List, E.J., Koh, R.C.Y., Imberger, J., Brooks, N.H., 1979. Mixing in Inland and Coastal Waters, Academic Press, San Diego, CA.

Forsman, K.J., 2000. Contaminant transport in non-uniform streams and streambeds. PhD Thesis, Uppsala University, Sweden.

Hart, D.R., Mulholland, P.J., Marzolf, E.R., DeAngelis, D.L., Hendricks, S.P., 1999. Relationships between hydraulic parameters in a small stream under varying flow and seasonal conditions. Hydrol. Process 13, 1497–1510.

Harvey, J.W., Fuller, C.C., 1998. Effect of enhanced manganese oxidation in the hyporheic zone on basin-scale geochemical mass balance. Water Resour. Res. 34 (4), 623–636.

Harvey, J.W., Wagner, B.J., Bencala, K.E., 1996. Evaluating the reliability of the stream tracer approach to characterize stream-subsurface water exchange. Water Resour. Res. 32 (8), 2444–2451.

Hollenbeck, K.J., 1998. INVLAP.M: a Matlab function for numerical inversion of Laplace transforms by the De Hoog algorithm. http://www.isva.dtu.dk/staff/karl/invlap.htm

Jackman, A.P., Walters, R.A., Kennedy, V.C., 1984. Transport and concentration controls for chloride, strontium, potassium and lead in Uvas Creek, a small cobble-bed stream in Santa Clara County, California, USA. 2. Mathematical modeling. J. Hydrol. 75, 111–141.

Jannasch, H.W., Honeyman, B.D., Balistrieri, L.S., Murray, J.W., 1988. Kinetics of trace element uptake by marine particles. Geochim. Cosmochim. Acta 52, 567–577.

Johansson, H., Jonsson, K., Forsman, K.J., Wörman, J., 2001. Retention of conservative and sorptive solutes in streams—simultaneous tracer experiment. Sci. Total Environ. 266/1-3, 229–238.

Jonsson, K., Wörman, A., 2001. Effect of sorption kinetics on the transport of solutes in streams. Sci. Total Environ. 266/1-3, 239–247.

Kaczynski, S.E., Kieber, R.J., 1993. Aqueous trivalent chromium photoproduction in natural waters. Environ. Sci. Technol. 27, 1572–1576.

Kaczynski, S.E., Kieber, R.J., 1994. Hydrophobic C_{18} bound organic complexes of chromium and their potential impact on the geochemistry of chromium in natural waters. Environ. Sci. Technol. 28, 799–804.

Kieber, R.J., Heiz, G.R., 1992. Indirect photoreduction of aqueous chromium(VI). Environ. Sci. Technol. 26, 307–312.

Lees, M.J., Camacho, L.A., Chapra, S., 2000. On the relationship of transient storage and aggregated dead zone models of longitudinal solute transport in streams. Water Resour. Res. 36 (1), 213–224.

Legrand-Marcq, C., Laudelout, H., 1985. Longitudinal dispersion in a forest stream. J. Hydrol. 78, 317–324.

Nyffeler, U.P., Li, Y.-H., Santschi, P.H., 1984. A kinetic approach to describe trace-element distribution between particles and solution in natural aquatic systems. Geochim. Cosmochim. Acta 48, 1513–1522.

Riise, G., Bjørnstad, H.E., Lien, H.N., Oughton, D.H., Salbu, B., 1990. A study on radionuclide association with soil components using a sequential extraction procedure. J. Radioanal. Nucl. Ch. 142 (2), 531–538.

Runkel, R.L., Kimball, B.A., McKnight, D.M., Bencala, K.E., 1999. Reactive solute transport in streams: a surface complexation approach for trace metal sorption. Water Resour. Res. 35 (12), 3829–3840.

Seo, I.W., Cheong, T.S., 2001. Moment-based calculation of parameters for the storage zone model for river dispersion. J. Hydr. Eng. 127 (6), 453–465.

Thibodeaux, L.J., Boyle, J.D., 1987. Bedform-generated convective transport in bottom sediment. Nature 325.

Wagner, B.J., Harvey, J.W., 1997. Experimental design for estimating parameters of rate-limited mass transfer: analysis of stream tracer studies. Water Resour. Res. 33 (7), 1731–1741.

Wörman, A., 1998. Analytical solution and timescale for transport of reacting solutes in rivers and streams. Water Resour. Res. 34 (10), 2703–2716.

Wörman, A., 2000. Comparison of models for transient storage of solutes in small streams. Water Resour. Res. 36 (2), 455–468.

Wörman, A., Forsman, J., Johansson, H., 1998. Modeling retention of sorbing solutes in streams based on tracer experiment using ^{51}Cr. J. Environ. Eng. 124, 122–130.